CORE
Metadata, citation and similar papers at core.ac.uk
Provided by Repositório Científico do Instituto Politécnico do Porto

Structure-function studies of BPP-BrachyNH2 and synthetic analogues thereof with Angiotensin I-Converting Enzyme

Daniel D.R. Arcanjo [a, b], Andreanne G. Vasconcelos [a], Lucas A. Nascimento [c, d], Ana Carolina Mafud [e, f], Alexandra Plácido [g], Michel M.M. Alves [b], Cristina Delerue-Matos [g], Marcelo P. Bemquerer [h], Nuno Vale [i], Paula Gomes [j], Eduardo B. Oliveira [k], Francisco C.A. Lima [d], Yvonne P. Mascarenhas [e], Fernando Aécio A. Carvalho [b], Ulf Simonsen [l], Ricardo M. Ramos [c, *, 1], José Roberto S.A. Leite [a, m, 1]

[a] Núcleo de Pesquisa Em Biodiversidade e Biotecnologia e BIOTEC, Campus Ministro Reis Velloso e CMRV, Universidade Federal do Piauí, UFPI, 642020-020, Parnaíba, PI, Brazil
[b] Núcleo de Pesquisas Em Plantas Medicinais e NPPM, Universidade Federal do Piauí e UFPI, Campus Ministro Petrônio Portella, SG-15, Ininga, 64049-550, Teresina, PI, Brazil
[c] Laboratório de Pesquisa Em Sistemas de Informaça-o, LaPeSI, Departamento de Informaça-o, Ambiente, Saúde e Produça-o Alimentícia, Instituto Federal do Piauí, Teresina, Brazil
[d] Grupo de Química Quântica Computacional e Planejamento de Fármaco, GQQCPF, Departamento de Química, Universidade Estadual do Piauí, Teresina, Brazil
[e] Instituto de Física de Sa-o Carlos e IFSC, Universidade de Sa-o Paulo e USP, Sa-o Carlos, SP, Brazil
[f] Department of Medical Parasitology and Infection Biology, Swiss Tropical and Public Health Institute, Basel, Switzerland
[g] LAQV/REQUIMTE, Instituto Superior de Engenharia do Instituto Politecnico do Porto, Rua Dr. Antonio Bernardino de Almeida, 431, 4200-072, Porto, Portugal
[h] EMBRAPA Recursos Geneticos e Biotecnologia, Parque Estaça-o Biológica, PqEB, Av. W5 Norte (final), 70770-917, Brasília, DF, Brazil
[i] UCIBIO/REQUIMTE, Laboratório de Farmacologia, Departamento de Ciências do Medicamento, Faculdade de Farmácia da Universidade do Porto, Rua de Jorge Viterbo Ferreira, 228, 4050-313, Porto, Portugal
[j] LAQV/REQUIMTE, Departamento de Química e Bioquímica, Faculdade de Ciências da Universidade do Porto, Rua do Campo Alegre, 687, 4169-007 Porto, Portugal
[k] Departamento de Bioquímica e Imunologia, Universidade de Sa-o Paulo, Ribeira-o Preto, Sa-o Paulo, 14096000, Brazil
[l] Department of Biomedicine, Pulmonary and Cardiovascular Pharmacology, Aarhus University, Aarhus, Denmark
[m] Area de Morfologia, Faculdade de Medicina, Universidade de Brasília, UnB, Brasília, DF, Brazil

Abstract

The vasoactive proline-rich oligopeptide termed BPP-BrachyNH2 (H-WPPPKVSP-NH2) induces *in vitro* inhibitory activity of angiotensin I-converting enzyme (ACE) in rat blood serum. In the present study, the removal of N-terminal tryptophan or C-terminal proline from BPP-BrachyNH2 was investigated in order to predict which structural components are important or required for interaction with ACE. Furthermore, the toxicological profile was assessed by *in silico* prediction and *in vitro* MTT assay. Two BPP-BrachyNH2 analogues (des-Trp^1-BPP-BrachyNH2 and des-Pro^8-BPP-BrachyNH2) were synthesized, and *in vitro* and *in silico* ACE inhibitory activity and toxicological profile were assessed. The des-Trp^1-BPP-BrachyNH2 and des-Pro^8-BPP-BrachyNH2 were respectively 3.2- and 29.5-fold less active than the BPP-BrachyNH2- induced ACE inhibitory activity. Molecular Dynamic and Molecular Mechanics Poisson-Boltzmann Surface Area simulations (MM-PBSA) demonstrated that the ACE/BBP-BrachyNH2 complex showed lower binding and van der Wall energies than the ACE/des-Pro^8-BPP-BrachyNH2 complex, therefore having better stability. The removal of the N-terminal tryptophan increased the *in silico* predicted toxicological effects and cytotoxicity when compared with BPP-BrachyNH2 or des-Pro^8-BPP-BrachyNH2. Otherwise, des-Pro^8-BPP-BrachyNH2 was 190-fold less cytotoxic than BPP-BrachyNH2. Thus, the removal of C- terminal proline residue was able to markedly decrease both the BPP-BrachyNH2-induced ACE inhibitory and cytotoxic effects assessed by *in vitro* and *in silico* approaches. In conclusion, the aminoacid sequence of BPP-BrachyNH2 is essential for its ACE inhibitory activity and associated with an acceptable toxico- logical profile. The perspective of the interactions of BPP-BrachyNH2 with ACE found in the present study can be used for development of drugs with differential therapeutic profile than current ACE inhibitors.

Keywords:
Docking; Molecular dynamics simulations; Molecular mechanics; Poisson-Boltzmann surface area g_mmpbsa proline-Rich oligopeptide; Toxicological prediction

1. Introduction

The study of poisons and toxins from animals as a source of new drugs for treatments for cardiovascular diseases has been consid- ered promising since the discovery of the proline-rich oligopep- tides (PRO) from the venom of *Bothrops jararaca* (Wied-Neuwied, 1824) [1]. A large number of studies have focused on the identifi- cation and characterization of novel PROs not only from the snake venom of *B. jararaca* but also from a variety of other natural sources, as well as on the identification of new biological targets for the PROs [2e4]. A list of 59 PROs previously described from different sources is shown in Table S1 (Supporting Information).

There is a large number of proline-rich oligopeptides (PROs) obtained from animal venom which have cardiovascular properties. Among them, the bradykinin-potentiating peptides (BPPs) invari- ably present a proline residue at the C-terminus, and are natural inhibitors of the angiotensin-converting enzyme (ACE), a zinc metallopeptidase that converts inactive angiotensin I to the vaso- constrictor peptide angiotensin II, and which catalyzes the hydro- lysis of bradykinin (BK). The ACE presents two homologous domains (N and C) with a catalytic site present in each one, which may be differentially active in the several isoforms of the enzyme. The description of the active sites and their role in the hydrolysis of various physiological substrates is of great importance, so that subtle variations of specific amino acid residues in their substrates influence the catalytic specificity of the C- and N-domain [2,5,6]. Araújo (2000) found that peptides with hydrophobic residues at the P_1 position and peptides with bulky groups in the P_2 position
are preferably hydrolyzed in the C-domain of ACE, such as occurs in
angiotensin I [7,8]. This information is also important for the un- derstanding of characteristics required for inhibitors of ACE.

Recently, our group demonstrated that BPP-BrachyNH$_2$, a novel proline-rich oligopeptide isolated from the skin secretion of the frog *Brachycephalus ephippium* with the primary structure H- WPPPKVSP-NH$_2$, evokes endothelium-dependent vasodilatation mediated by NO [9]. Also in this work, *in silico* molecular modeling and docking studies suggested that BPP-BrachyNH$_2$ has the ability of forming a hydrogen bond network and also multiple van der Waals interactions with human ACE. They suggest that the peptide creates an impediment for the substrate to the active C-domain site of ACE. BPP-BrachyNH$_2$ has a different primary structure in com- parison to other BPPs, but it still has an inhibitory effect on ACE activity. Therefore, structure-function studies involving BPP-Bra- chyNH$_2$ and synthetic analogues thereof are of interest to reveal the interactions of the peptide with ACE. In this context, structure- activity relationships studies are important to infer mechanisms of action, being an important tool to rational development of new drugs which are more efficient and highly selective. For example, peptides from *B. jararaca* venom gave information allowing to analyze and understand the structureefunction relationships as well as the design of efficient and potent analogues with effect by oral administration, such as captopril, an ACE inhibitor with anti-hypertensive effect [10,11].

In this work, the removal of N-terminal tryptophan or C-terminal proline from BPP-BrachyNH$_2$ was proposed in order to predict which structural components are important or required for interaction with ACE, and then to promote the inhibitory effect. Two BPP-BrachyNH$_2$ analogues, des-Trp^1-BPP-BrachyNH$_2$ and des-Pro^8-BPP-BrachyNH$_2$ were synthesized, and their cytotoxicity and
in vitro ACE inhibitory activity in rat blood serum were assessed. Furthermore, *in silico* studies were also performed in order to predict toxicological targets and effects, as well as to analyze the interaction of peptides and captopril with ACE.

2. Material and methods

2.1. Synthesis, purification and characterization of BBP-BrachyNH$_2$ and synthetic analogues

The synthesis of the BPP-BrachyNH$_2$ (H-WPPPKVSP-NH$_2$), des- Trp^1-BPP-BrachyNH$_2$ (H-PPPKVSP-NH$_2$), and des-Pro^8-BPP-Bra- chyNH$_2$ (H-WPPPKVS-NH$_2$) were carried out manually, with a
standard F-moc (N-(9-fluorenyl)methoxycarbonyl) chemistry starting from a Rink-amide-MBHA resin (0.59 mmol.g-1, Peptides International, Louisville, KY, USA) [12]. F-moc-protected amino acid derivatives (Peptides International, Louisville, KY, USA) were used in four-fold molar excess relative to the nominal scale of synthesis (1.2 mmol). Couplings were performed with 1,3- diisopropylcarbodiimide/ethyl 2-cyano-2-(hydroxyimino) acetate (DIC/Oxyma) in N,N-dimethylformamide (DMF) for 2e3 h. Side chain protected groups were *tert*-butyl for Ser, and Boc for Lys and Trp. Amino group deprotection was conducted by 4- methylpiperidine/DMF (1:4, v:v) for 20e30 min. Removal of side chain protection and cleavage of the peptides from the resin were performed by the use of 10.0 mL TFA:water:tioanisol:ethanodi-thiol:triisopropylsilane (86:5.0:5.0:2.5:1.0, v:v:v:v:v) with addition of 1 g phenol for 90 min at room temperature under shaking. After solvent evaporation under nitrogen, the peptides were precipitated by addition of cold diisopropyl ether, collected by filtration and washed four times with cold diisopropyl ether. Extraction was
performed with 200 mL H_2O:ACN (1:1, v:v) and crude peptides were lyophilized. Purification was performed using a preparative HPLC system (LaPrep Sigma), with LP1100 Quaternary LPG pump injection with fractionation valve. The elution conditions consisted of a linear gradient from 10% to 30% of acetonitrile in water. The effluent was monitored at the absorbance of 220 nm, absorbing products were collected, and the peptides were lyophilized and analyzed by MALDI-TOF MS and MS/MS HPLC and LC-MS. Purified
peptides with 98% purity were obtained. Stock peptide solutions were prepared in water and their concentrations were determined according to tryptophan molar absorptivity (5550 M^{-1} cm^{-1}) at
280 nm, when applicable [9].

2.2. In vitro Angiotensin I-Converting enzyme (ACE) inhibition assay

2.2.1. Animals

Fresh blood sera were obtained from male Wistar rats

(250e300 g, 3 months) according to Arcanjo et al. (2015) [9]. The animals were maintained throughout the study period at 12 h light/ dark cycle and temperature of 23 ± 2 °C), with free access to water and food (Purina-Nestlę, Sao Paulo, SP, Brazil). The experimental procedures were performed with approval by the Ethics Committee for Animal Experimentation from the Federal University of Piauí, Brazil (permission No. 008/2012).

2.2.2. ACE inhibition assay

The ACE-inhibition assay was performed according to Arcanjo et al. (2015) [9]. Briefly, fresh Wistar rat serum as source of ACE, 1.0 mM H-hippuryl-His-Leu-OH as ACE substrate, and different concentrations of BPP-BrachyNH$_2$ (0.05e50 mM), des-Trp^1-BPP- BrachyNH$_2$ (0.3e600 mM), des-Pro^8-BPP-BrachyNH$_2$ (500e1.9 mM) and captopril (0.12e2000 nM) were incubated at 37 °C for 20 min. The reaction was carried out in duplicate, at 20 mM Tris buffer in 0.3 M NaCl (200 mL), pH 8.1, and interrupted by 1 mL of 0.5 M NaOH. The product H-His-Leu-OH was derivatized with *o*-phtaldialdehyde in 4 min of reaction. Thereafter, 200 mL 6.0 M HCl were added, and the mixture was centrifuged in order to remove precipitated pro- teins. The product from ACE-catalyzed hydrolysis was measured fluorimetrically, and the IC_{50} values (concentration of the inhibitor that results in 50% of maximal activity) were determined using non-linear regression derived from concentration-response curves plotted as a function of each inhibitor.

2.3. In silico interaction studies with Angiotensin I-Converting enzyme (ACE)

2.3.1. Peptides and captopril setup

All calculation and drawing were carried out using Gaussian 09W version 7.0 packages molecular mechanics methods [13]. The captopril 3D structure was downloaded from PubChem Open Chemistry Database (https://pubchem.ncbi.nlm.nih.gov/) with the PubChem CID 44093 code. The initial structures of both peptides BBP-BrachyNH$_2$ and des-Pro^8-BBP-BrachyNH$_2$ were constructed by molecular builder of Gauss View version 5.0.8 [14] implemented in computational package Gaussian 09W version 7.0. The molecular structures of ligands (captopril and peptides) were fully optimized by PM3 semi empirical method without imposing any symmetrical restrictions [14]. All calculations of ligands in work were performed in vacuum. The behavior of the charge on the molecular structure was calculated by the Mulliken atomic charges using the Gaussian 09W. The topologies of ligands, necessary for molecular dynamics simulations, were generated from the pre-optimized atomic co- ordinates with the PRODRG program (http://davapc1.bioch.dundee. ac.uk/cgi-bin/prodrg) [15]. Atomic charges generated from PRODRG were substituted by atomic charges calculated with Gaussian 09W.

2.3.2. Docking

All docking procedures utilized the Autodock 4.2 package [16e18]. Protein (ACE) and ligands were prepared for docking simulations with AutoDock Tools (ADT), version 1.5.6 [19]. The receptor was considered rigid whereas each ligand was considered flexible. Gas- teiger [20] partial charges were calculated after addition of all hy- drogens. Nonpolar hydrogen atoms of protein and ligand were subsequently merged. A cubic box of 60 x 60 x 60 points with a spacing of 0.35 Å between the grid points was generated for the whole protein target. The grid box was centered on the Arg522 from ACE. The global search Lamarckian genetic algorithm (LGA) [21] and the local search (LS) pseudo-Solis and Wets [22] methods were applied in the docking search. Each ligand was subjected to 100 independent runs of docking simulations. The rest of the docking parameters were set as the default values. The resulting docked conformations were clustered into families according to the RMSD. The initial coordinates of ACE complexes for molecular dynamics simulations were chosen using the criterion of lowest docking conformation of the cluster with lowest energy combined with visual inspection.

2.3.3. Molecular dynamics simulations

Molecular dynamics simulations were carried out using GRO- MOS96 53a6 force field [23] implemented in GROMACS package version 4.6.7 [24]. All systems were simulated in NPT ensemble (wherein the Number of particles, Pressure, and Temperature are all constant) and periodic boundary conditions (cubic). The dimensions of the central box were chosen in such way that the minimum dis- tance of any protein atom to the closest box wall was 12 Å. The simulations were carried out using explicit solvent water molecules described by the simple point charge (SPC) model [25]. The total charge of the systems was -13 for the three complexes (ACE/BPP- BrachyNH$_2$, ACE/des-Pro^8-BPP-BrachyNH$_2$ and ACE/captopril). So- dium ions were added to neutralize each system. Initially, the pro- tein structure in each system was submitted to a maximum of 50000 steps of steepest descent energy minimization. To relax strong solvent-solvent and solvent-protein non-bonded interactions, 100 ps of MD simulation was performed restraining the protein struc- ture. Initial velocities were assigned according to Maxwell distri- bution. The simulations were performed for 10 ns using an integration time step of 2 fs. Each system was heated with gradual increments in the following temperatures: 100 K (10 ps),150 K (5 ps), 200 K (5 ps), and 250 K (5 ps). After these steps, the temperatures of the systems were adjusted to 310 K. The first 6 ns of each simulation was considered as part of the heating (0.025 ns) and the equilibra- tion (5.975 ns) steps and had not been used in the data analysis. The temperatures of solvent and solutes (protein, ligands, water and sodium ions) were independently coupled to a thermal bath with a relaxation time of 0.1 ps using the V-rescale thermostat. The pres- sure in the systems was weakly coupled to a pressure bath with 2 ps of relaxation time using the Parrinello-Rahman barostat [26,27]. Bond lengths were constrained using the LINCS algorithm [28] with 4th order expansion. Electrostatic interactions among non-ligand atoms were evaluated by the PME (Particle Mesh Ewald) method [29] with a charge grid spacing of approximately 1.0 Å. The charge grid was interpolated on a cubic grid with the direct sum tolerance set. Lennard-Jones interactions were evaluated using a 14 Å atom- based cutoff. The pair list was updated at each ten steps.

To increase sampling, all ACE-ligand complex MD simulations were run thrice for 10 ns using different starting atomic velocities assuming a Maxwellian distribution. A total of nine simulations were performed. Data generated during the last 4 nanoseconds of each simulation system, the period defined as the production stage, were used for analysis. A total of 123 snapshots, each taken every 100 ps,
were obtained for each complex during the production stage. Where applicable, detailed interactions were calculated using the LigPlot[þ]
program [30]. A minimum binding of 50% of contacts (sum of hy- drophobic interactions and hydrogen bonds) in the analyzed frames was established as the criterion for binding efficiency [31]. Of the three simulations of each complex (ACE/BPP-$BrachyNH_2$, ACE/des-
Pro^8-BPP-$BrachyNH_2$ and ACE/captopril) were selected for analysis
with g_mmpbsa program (section 2.4) simulation with more con- tacts both by hydrogen bonds and hydrophobic interactions.

2.3.4. *Molecular mechanics Poisson-Boltzmann surface area MM- PBSA*

The MM/PBSA binding energy was calculated with the g_mmpbsa program (http://rashmikumari.github.io/g_mmpbsa/) for the last 4 nanoseconds of MD simulations [32]. In this work, g_mmpbsa program used the GROMACS software version 4.6.7 and APBS (Adaptive Poisson-Boltzmann Solver) version 1.4.1 [33]. The binding energy consists of three energetic terms, potential energy in vacuum, polar-solvation energy and non-polar solvation energy.
The vacuum, solvent and solute dielectric constants were set at 1, 80 and 2, respectively. The calculation of non-polar solvation energy was based on SASA model. The entropy contribution was not included in the calculation of binding energy.

2.4. *In silico toxicity prediction*

The peptides were designed according to the FASTA query peptide by AMMP, a full-featured molecular dynamics program to manipulate both small molecules and macromolecules including proteins, nucleic acids and other polymers [34]. The Ammp-Mon charges were added and AMBER field force was applied to minimize the energy conformation, through a genetic algorithm, with 3000 steps. The conformational search was performed by using the Boltzmann jump method, with flexible and psi torsions, at 300 K, with dielectric constant equal to 80,000 and RMSD equal to 60.00. The toxicity prediction for BPP-$BrachyNH_2$ and its analogues des-Trp^1-BPP-$BrachyNH_2$ and des-Pro^8-BPP-$BrachyNH_2$ was performed by pkCSM. This analysis is based on the *in silico* determination of several predictors, such as human maximum tolerated dose, oral rat acute toxicity (LD_{50}), oral rat chronic toxicity, human ether-à-go-go related gene (hERG) inhibitors, hepatotoxicity, skin sensitization and mutagenicity [35]. Other physicochemical properties were also calculated, such as molecular weights (MW), lipophilicity (logP), rotatable bonds (NRB), polar surface area (PSA), number of hydrogen bond acceptors (HBA) and number of hydrogen bond donors (HBD).

2.5. *Cytotoxicity assessment*

2.5.1. *Animals and cell cultures*

Peritoneal macrophages were obtained from male BALB/c mice (25e30 g, 2 months) according to Rodrigues et al. (2015) [36]. The animals were maintained throughout the study period at 12 h light/dark cycle and temperature of 23 ± 2 °C), with free access to water and food (Purina-Nestlé, São Paulo, SP, Brazil). For the hemolysis assay, red blood cells were obtained by centrifugation of sheep (9 months-old) blood. The experimental procedures were performed with approval by the Ethics Committee for Animal Experimentation from the Federal University of Piauí, Brazil (permission No. 008/2012).

2.5.2. *Cell viability assay on murine macrophages*

The evaluation of the cytotoxic activity of BPP-$BrachyNH_2$, des-Trp^1-BPP-$BrachyNH_2$ and des-Pro^8-BPP-$BrachyNH_2$ on BALB/c murine macrophages was performed by MTT assay as previously described [37]. Briefly, the peptides were incubated at different concentrations (10^{-7}, 5×10^{-7}, 10^{-6}, 5×10^{-6}, 10^{-5}, 5×10^{-5}, 10^{-4} and 5×10^{-4} M) with macrophages (1×10^6/well) during 48 h in RPMI 1640 medium (Sigma, St. Louis, USA) at 37 °C and 5% CO_2. Thereafter, MTT (3-[4,5-dimethylthiazol-2-yl]-2,5-diphenyltetrazolium bromide) was incubated during 4 h. The absorbance values were read at 550 nm (ELx800™, BioTek® Instruments, USA). Concentration-response curves were fitted using non-linear regression (GraphPad Prism version 6.00 for Windows, GraphPad Software, La Jolla California USA, www.graphpad.com), and the mean cytotoxic concentrations (CC_{50}) were determined.

2.5.3. *Hemolysis assay on sheep blood erythrocytes*

The hemolytic activity was assessed by incubating 80 mL of 5.0% fresh sheep red blood cells in PBS with 20 mL of different concen- trations of BPP-$BrachyNH_2$, des-Trp^1-BPP-$BrachyNH_2$ and des-Pro^8- BPP-$BrachyNH_2$ (10^{-6}, 5×10^{-6}, 10^{-5}, 5×10^{-5} and 10^{-4} M) at 37 °C
for 1 h. After addition of 200 mL of PBS, the suspensions were centrifuged at 1000 × g for 10 min, and the hemolysis was measured at 540 nm (ELx800™, BioT ® Instruments, USA). The blank control and maximal lysis (positive control) were obtained by replacing the substance sample with equal volume of PBS or distilled water, respectively [38].

3. Results

3.1. Synthesis, purification and characterization

The positive ionization MALDI *m/z* spectra (Fig. S1), and peptide fragmentation and sequencing by mass spectrometry (Fig. S2) obtained for the peptides BPP-BrachyNH$_2$ and analogues confirmed the molecular weights and amino acid sequence, as follows: BPP-BrachyNH$_2$: H-WPPPKVSP-NH$_2$; [MþH^þ] ¼ 906.92; des-Trp^1-BPP-BrachyNH$_2$: H-PPPKVSP-NH$_2$; [MþH^þ] ¼ 720.82); and des-Pro^8-BPP-BrachyNH$_2$: H-WPPPKVS-NH$_2$; [MþH^þ] ¼ 809.91.

3.2. In vitro ACE inhibition assay

The inhibitory effect of BPP-BrachyNH$_2$, the analogues thereof and captopril on rat serum ACE activity, as well as their IC$_{50}$ values are shown in Fig. 1. The removal of the N-terminal tryptophan decreases by 3.2-fold the inhibition of ACE activity by BPP-Bra- chyNH$_2$. The removal of C-terminal proline residue from BPP-BrachyNH$_2$ decreased also significantly the inhibitory effect of ACE. The analogue des-Pro^8-BPP-BrachyNH$_2$ was 29.5-fold less active when IC$_{50}$ values were compared with those of BPP-BrachyNH$_2$.

3.3. In silico interaction studies

The crystal structure of the C-domain ACE (PDB code: 3BKK) was obtained from the Protein Data Bank. Molecular dockings of ligands (BPP-BrachyNH$_2$, des-Pro^8-BPP-BrachyNH$_2$ and captopril) with the 3D structure of ACE were based on Arg522 (the active site residue) [39]. Table 1 shows the results of docking. Positive values for ΔG_{bind} were observed for association with the peptides (32.78 kcal/mol to ACE/BPP-BrachyNH$_2$ and 24.70 kcal/mol for ACE/des-Pro^8-BPP-BrachyNH$_2$), which can be explained by the volume of the peptides that does not favor staying in the ACE active site region. The ACE/captopril complex has a binding energy of -7.67 kcal/mol which is in agreement with the literature since captopril is a known ACE inhibitor. BPP-BrachyNH$_2$ formed hydrogen bonds with three amino acid residues (Arg522, Met223, Tyr523) and hydrophobic interactions with fifteen amino acid residues. The des-Pro^8-BPP-BrachyNH$_2$ analogue formed hydrogen bonds with one amino acid residue (Tyr523) and hydrophobic interactions with sixteen amino acid residues. Captopril formed hydrogen bonds with four amino acid residues (His353, His513, Tyr520, Lys511) and hydrophobic interactions with eight amino acid residues. It is also observed that the ligands remained in the active site region and formed interactions with Tyr523 from the enzyme. Fig. 2 shows a graphical representation of conformations resulting from docking.

With the conformations resulting from docking three MD simulations were carried out for each complex (ACE/BPP-BrachyNH$_2$, ACE/des-Pro^8-BPP-BrachyNH$_2$ and ACE/captopril), giving rise to a total of nine simulations. Fig. 3 shows the frequency of contacts of ligands with the ACE. The interactions were calculated for frames extracted from the last 4 ns of the MD simulations using the LigPlot^þ program. A criterion efficiency of a minimum of 50% of contacts (sum of hydrophobic interactions and hydrogen bonds) in the analyzed frames was established.

It is observed that the frequency of BPP-BrachyNH$_2$ contacts with ACE (Fig. 3A) was higher by hydrophobic interactions (Trp220, Glu123, Ser517, Leu122, Met223, His353, Glu403, Ser 219, Ser355, His410, Ala354 and Arg522 - green bars) than by hydrogen bonds

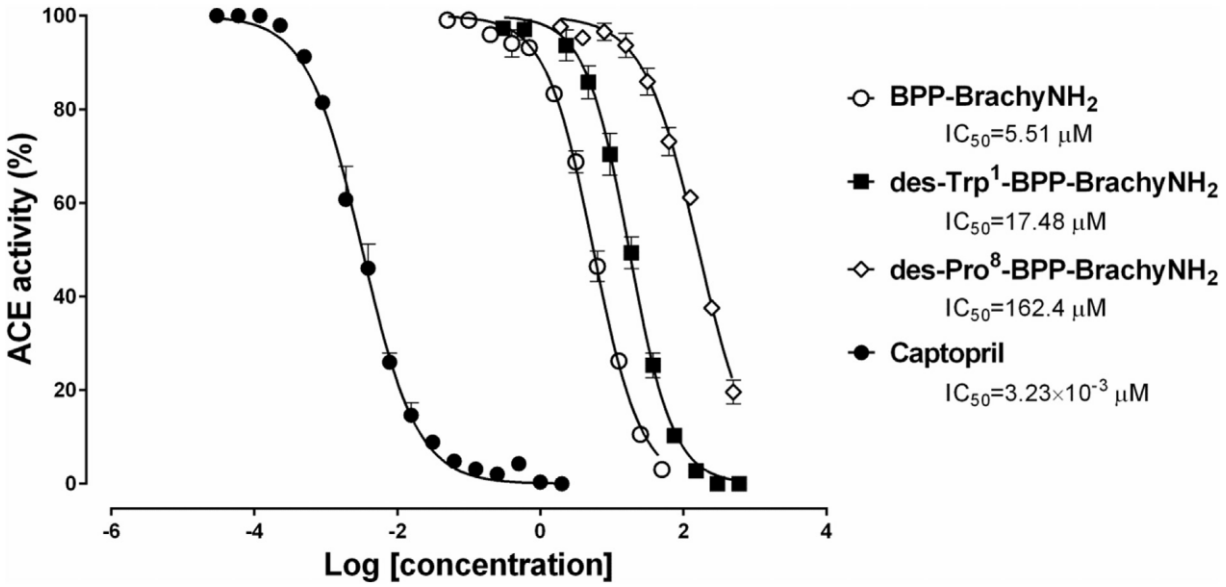

Fig. 1. Inhibitory effect of BPP-BrachyNH$_2$, des-Trp^1-BPP-BrachyNH$_2$ and des-Pro^8-BPP-BrachyNH$_2$ and Captopril on rat serum angiotensin converting enzyme (ACE) activity. Residual enzymatic activities are plotted against the corresponding inhibitor concentrations. The IC_{50} values were calculated by non-linear regression using GraphPad Prism 6.00 software.

Table 1
Parameters affinity of the molecular docking.

Complex (Protein-ligand)	DG_{bind}[a] (kcal/mol)	Number of independent docking runs	Number of conformations in the first ranked cluster	Amino acids that interact through hydrogen bonds[b]	Amino acids that make hydrophobic interactions[b]
ACE/BPP-BrachyNH$_2$	38.78	100	02	Arg522, Met223, Tyr523	Glu123, Trp220, Ser219, Pro407, Gly404, Asn406, Glu403, His410, Ser355, His387, Ala356, Glu411, Val518, Pro519, Ile204
ACE/des-Pro^8-BPP-BrachyNH$_2$	24.70	100	07	Tyr523	Ser516, Phe512, His353, Val518, His513, Val380, Asp415, Phe527, Phe457, His383, Glu411, Glu384, Ala356, His387, Ser355, Ala354
ACE/Captopril	-7.67	100	100	His353, His513, Tyr520, Lys511	His383, His387, Glu411, Tyr523, Ala354, Phe457, Gln281, Glu384

[a] Binding energy of the best conformation.
[b] Obtained with the Ligplotþ software.

(Arg522, Ala354, Ser 219, His410, Ser517, Trp220, Glu123 and Glu403 - orange bars). Trp220 (93%) and Arg522 (58%) were the residues with higher frequencies of contacts by hydrophobic interactions and hydrogen bonds, respectively. All amino acid residues that made contacts by hydrogen bonds also establish hydrophobic interactions. It is also observed that Arg522 has a total frequency of 68% interactions (58% by hydrogen bonds and 10% by hydrophobic interactions).

In Fig. 3B, it is also observed that the interaction of des-Pro^8-BPP-BrachyNH$_2$ with ACE was more frequent by hydrophobic interactions (Leu132, Tyr62, Leu81, Lys84, Asn85, Ala129, Ala89, Ala65, Met86, Gln87, Asn136) than by hydrogen bonds (Met86, Asn136, Ile88, Gln87, Ala89, Asn85, Lys84, Ala129 and Tyr62). The Ile88 residue (52% frequency) showed only contacts by hydrogen bonds with ACE. Leu132 (81%) and Met86 (55%) were the residues with higher frequencies of contacts by hydrophobic interactions and hydrogen bonds, respectively. Also, Met86 is observed that has a total frequency of 92% (55% by hydrogen bonds and 37% by hydrophobic interactions).

The frequency of captopril contacts with ACE (Fig. 3C) as well as the previous ligands was higher by hydrophobic interactions (Phe457, Tyr523, His513, His383, His353, Ala354, Tyr520, Lys511 and Gln281) than by hydrogen bonds (Gln281, Lys511, Tyr520, Ala354, His513, Tyr523, His353 and His383). Phe457 (89%) and Tyr523 (89%) were the residues with higher frequencies of contacts by hydrophobic interactions. Gln281 (43%) was the residue with greater frequency of contact by hydrogen bonds. It is also observed that the Tyr523 enzymatic residue has a total frequency of 96% (7% by hydrogen bonds and 89% by hydrophobic interactions).

Fig. 4 shows the binding mode of ligands after docking (yellow) and after MD simulations (green) and takes into account the three MD simulations that were carried out for each complex simulation with higher contact by hydrogen bonds and hydrophobic interactions. It is observed that the BPP-BrachyNH$_2$ remained close to Arg522 in the active site region after the MD simulation (see Fig. 4A-1, 4A-2 and 4A-3). On the other hand, des-Pro^8-BPP-BrachyNH$_2$ shifted to the end of the ACE after the MD simulation, coming out of the active site region, and making interactions with amino acid residues that are located on the surface as Leu132 and Met86. It is also observed that a part of des-Pro^8-BPP-BrachyNH$_2$ is out of ACE, indicating the exit from the protein (see Fig. 4B-1, 4B-2 and 4B-3). Captopril, such as BPP-BrachyNH$_2$, remained in the active site region after MD simulations (see Fig. 4C-1, 4C-2 and 4C-3). The positions of the ligands to MD simulations were not very close to the position of the ligands shown in Fig. 4 (data not shown).

Table 2 shows the results of binding energies of the complex

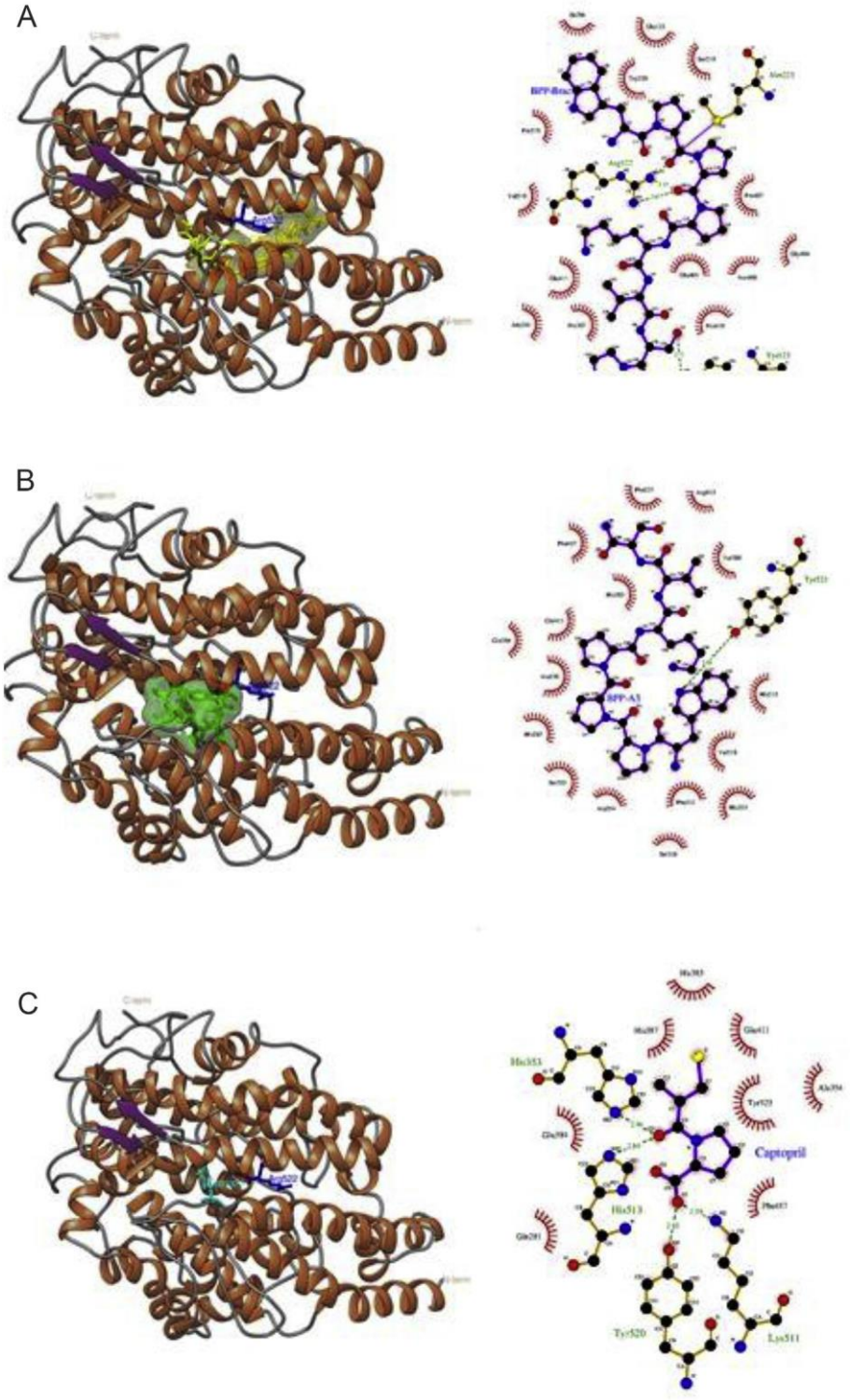

Fig. 2. Global structure of the conformations results from docking. Left hand panels: schematic representation of structure of BPP-BrachyNH$_2$ (A), des-Pro^8-BPP-BrachyNH$_2$ (C) and captopril (E); Right-hand panels: LIGPLOT diagrams for ligands interaction in BPP-BrachyNH$_2$ (B), des-Pro^8-BPP-BrachyNH$_2$ (D) and captopril (F). ACE represented by ribbons. Ligands (BPP-BrachyNH$_2$ - yellow, des-Pro^8-BPP-BrachyNH$_2$ - green, and Captopril - cyan) and Arg522 (blue) represented by sticks. Figure were generated using UCSF Chimera (https://www.cgl.ucsf.edu/chimera/) [40].

obtained by g_mmpbsa. It is observed that the ACE/BBP-BrachyNH$_2$ complex showed lower binding energy ($DG_{binding}$ ¼ -134.187 ± 18.112 kJ/mol) compared to other complexes. The energy of van der Wall was lower for ACE/BBP-BrachyNH$_2$ complex (D_{EvdW} ¼ -291.834 ± 12.151 kJ/mol), which is in accordance with the frequency of contacts (Fig. 3) because this complex showed a higher number of hydrophobic interactions. Electrostatic energy for ACE/des-Pro^8-BPP-BrachyNH$_2$ complex (DE_{elec} ¼ -75.411 ± 30.200 kJ/mol) was more favourable than for the ACE/BPP-BrachyNH$_2$ complex (DE_{elec} ¼ -69.756 ± 14.936 kJ/

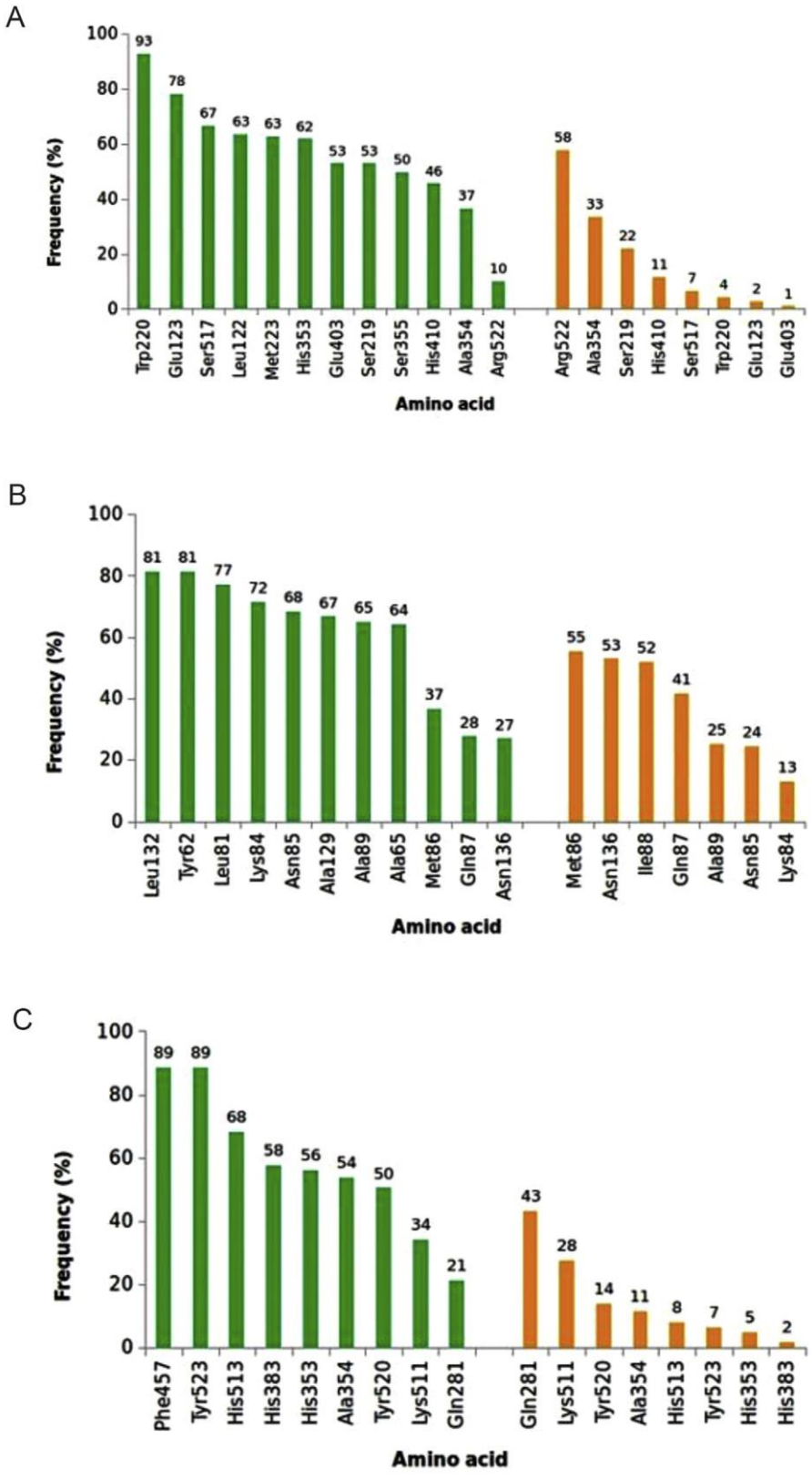

Fig. 3. Identified contacts between the ligands and ACE calculated for the last 4.0 ns of MD simulations. (A) BPP-Brachy, (B) des-Pro^{8}-BPP-BrachyNH_2, and (C) Captopril. Color system: hydrophobic interactions (green) and hydrogen bonds (orange). The numbers on the bars indicate the percentage of contacts for each amino acid residue. Contacts evaluated on snapshots taken every 100 ps of the production stage. (For interpretation of the references to colour in this figure legend, the reader is referred to the web version of this article.)

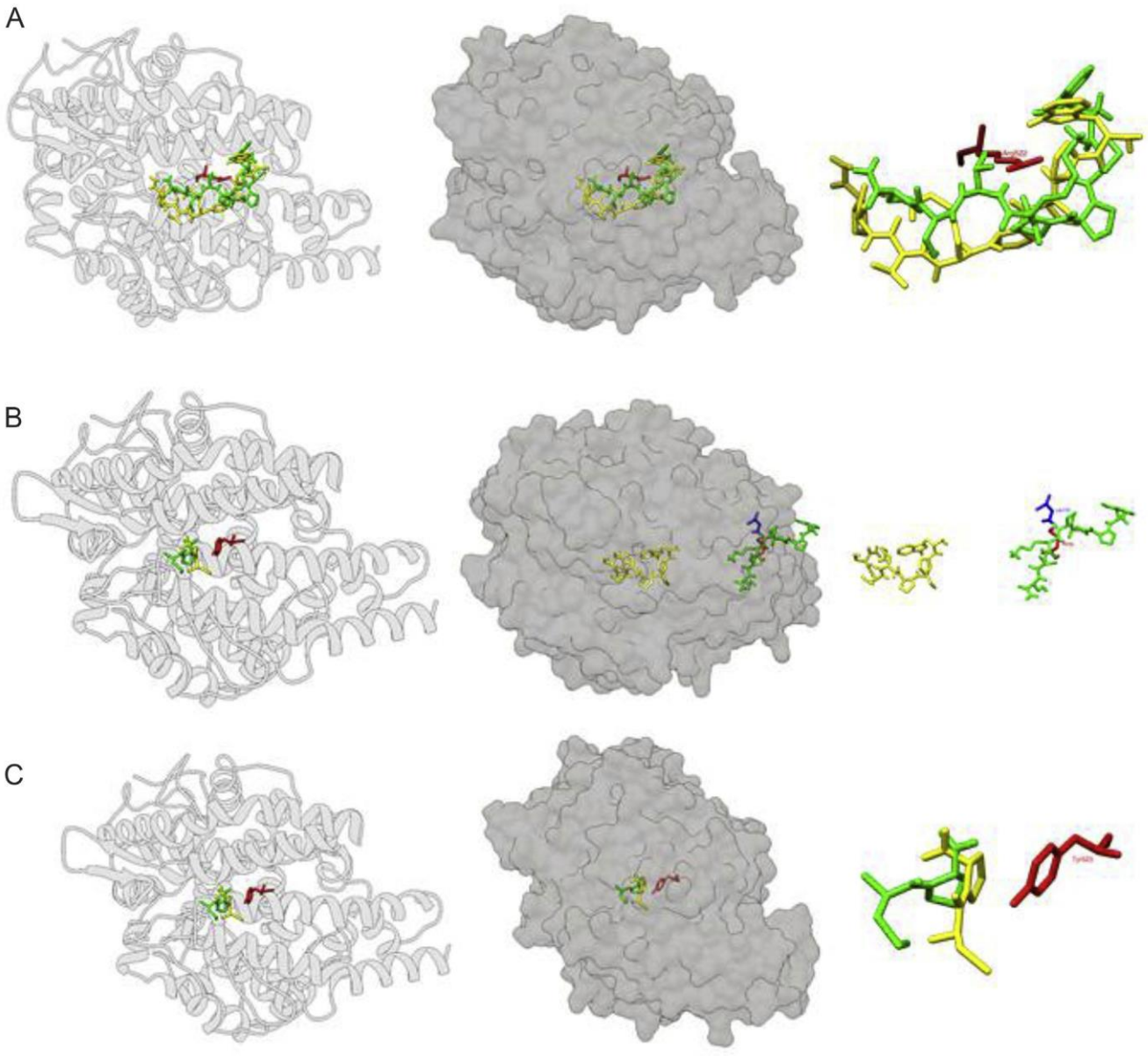

Fig. 4. Global structure of the complexes and binding mode of ligands calculated for docking (yellow) and for the last frame of MD simulations (green). BPP-BrachyNH_2 (A1, A2 and A3). Des-Pro^8-BPP-BrachyNH_2 (B1, B2, and B3). Captopril (C1, C2 and C3). Left hand panels: ACE represented by transparent ribbons, residues and ligands by sticks; Central panels: ACE represented by transparent surface, residues and ligands by sticks; Right-hand panels: expansion of the binding mode of ligands on ACE and residues more frequently contacts (see Fig. 3) represented by sticks. (For interpretation of the references to colour in this figure legend, the reader is referred to the web version of this article.)

Table 2
Binding energies of protein-ligand complexes obtained by g_mmpbsa.

Complex (Protein-ligand)	DE_{vdW}[a]	DE_{elec}	DG_{polar}	$DG_{nonpolar}$	$DG_{binding}$
ACE/BPP-BrachyNH_2	-291.834 ± 12.151	-69.756 ± 14.936	259.122 ± 22.788	-31.720 ± 1.531	-134.187 ± 18.112
ACE/des-Pro^8-BPP-BrachyNH_2	-227.404 ± 17.630	-75.411 ± 30.200	241.689 ± 32.929	-27.775 ± 2.355	-88.901 ± 23.614
ACE/Captopril	-101.550 ± 10.066	-34.782 ± 16.670	112.223 ± 32.109	-11.178 ± 0.819	-35.287 ± 21.169

[a] DE_{vdW}, DE_{elec}, DG_{polar}, and $DG_{nonpolar}$ are binding energy components of van der Waals, electrostatic, polar and nonpolar solvation energies, respectively. $DG_{binding}$ is the total binding energy. The unit of energy is kJ/mol.

mol) as the first one has a higher number of hydrogen bonds according to the frequency of contacts (Fig. 3). The large difference in the binding energy of the BPP-BrachyNH_2 when compared with des-Pro^8-BPP-BrachyNH_2 is due to the fact the latter compound has much of its structure outside the ACE without making interactions with it. Captopril, a known ACE inhibitor, showed an expected favourable value for the binding energy ($DG_{binding}$ ¼ -35.287 ± 21.169 kJ/mol) according to the literature.

3.4. *In silico toxicity prediction*

In this study, the toxicity prediction for BPP-BrachyNH$_2$ and their analogues des-Trp^1-BPP-BrachyNH$_2$ and des-Pro^8-BPP-BrachyNH$_2$ were assessed. The BPP-BrachyNH$_2$ is well-tolerated by humans and rats, as well as the AMES mutagenicity prediction and skin sensitization revealed negative results. On the other hand, the predicted mean lethal dose (LD_{50}) of des-Trp^1-BPP-BrachyNH$_2$ in oral rat acute and chronic toxicity seem to be slightly lower than either LD_{50} values for BPP-BrachyNH$_2$ or des-Pro^1-BPP-BrachyNH$_2$, probably indicating a higher toxic effect (Table 3).

3.5. *In vitro cytotoxicity assessment*

In these protocols, no hemolysis of sheep erythrocytes was observed for peptides, even at the highest assayed concentrations (data not shown). Besides, the incubation of peptides BPP-BrachyNH$_2$ and des-Trp^1-BPP-BrachyNH$_2$ promoted a concentration-dependent decrease of cell viability of macrophages (Fig. 5). Although no significant difference between respective CC_{50} values was observed, a point-by-point statistical comparison demonstrated that the removal of N-terminal Trp^1 residue increased the cytotoxicity at concentrations of 10^{-5} and 5×10^{-5} M (Fig. 5). On the other hand, the peptide des-Pro^8-BPP-BrachyNH$_2$ promoted only a slight significant decrease of cell viability by 7.7 and 14.8% at concentrations of 10^{-4} and 5×10^{-4} M, respectively (Fig. 5). The CC_{50} value calculated for des-Pro^8-BPP-BrachyNH$_2$ was 190-fold higher than CC_{50} value for BPP-BrachyNH$_2$.

4. Discussion

In the present study, the removal of N-terminal tryptophan or C-terminal proline from BPP-BrachyNH$_2$ was investigated in order to predict which structural components are important or required for the toxicological profile of BPP-BrachyNH$_2$ and its analogues was assessed by *in silico* prediction using pkCSM software and by MTT interaction with ACE, to promote the inhibitory effect. Furthermore,

Table 3
Physicochemical properties and toxicity predictions of BPP-BrachyNH$_2$ and their synthetic analogues.

Peptide properties (pH 7,4)			
Sequence	WPPPKVSP-NH$_2$	PPPKVSP-NH$_2$	WPPPKVS-NH$_2$
Length	8	7	808.4582
Mass (g/mol)	905.5108	719.4317	808.4582
Isoelectric point (pI)	13.88	14.00	13.88
Net charge	þ2	þ2	þ2
Hydrophobicity (Kcal/mol)	þ9.17	þ11.26	þ9.03
Extinction coefficient (1/M*cm)	5500	0	5500
LogP	-2.7149	-4.3146	-2.7059
Rotatable Bonds	26	22	24
Acceptors	9	8	8
Donors	8	7	8
Surface Area (Å^2)	378.597	298.843	337.857
Toxicity prediction			
AMES toxicity	No	No	No
Max. tolerated dose (human) (log mg/kg/day)	0.505	1.136	0.614
hERG I inhibitor	No	No	No
hERG II inhibitor	Yes	No	Yes
Oral Rat Acute Toxicity (LD_{50}) (mol/kg)	2.661	2.046	2.735
Oral Rat Chronic Toxicity (LOAEL) (log mg/kg_bw/day)	3.402	2.55	3.306
Hepatotoxicity	Yes	Yes	Yes
Skin Sensitization	No	No	No
T. pyriformis toxicity (log mg/L)	0.285	0.285	0.285
Minnow toxicity (log mM)	5.577	6.191	5.235

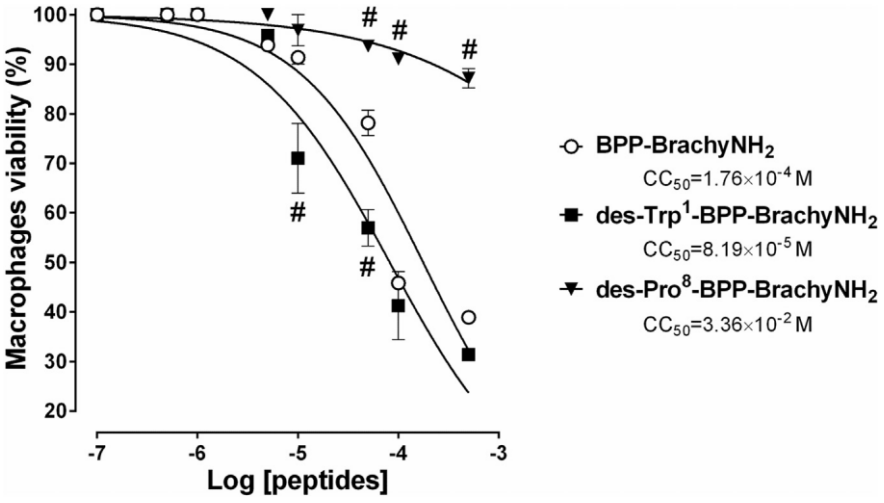

Fig. 5. Cytotoxicity of BPP-BrachyNH$_2$, des-Trp^1-BPP-BrachyNH$_2$ and des-Pro^8-BPP-BrachyNH$_2$ on BALB/c mice peritoneal macrophages by MTT test. The mean cytotoxic concentration (CC_{50}) was determined by non-linear regression. Data were expressed as mean cell viability (%) ± S.E.M. of experiments carried out in triplicate. $^{\#}p < 0.001$ *vs.* respective concentrations of BPP-BrachyNH$_2$.

assay in BALB/c peritoneal macrophages. The main finding of the present study was the BPP-BrachyNH$_2$-induced both ACE inhibitory and toxicological effects were both markedly decreased by removal of the C-terminal proline residue.

The BPP-BrachyNH$_2$-induced ACE inhibitory activity was consistent with previously reported results. A previous docking study has reported a higher interaction between BPP-BrachyNH$_2$ and C-domain rather than N-domain of ACE. The C-terminal Pro^8 residue from BPP-BrachyNH$_2$ established more interaction bonds with ACE than other residues at C-domain of ACE [9]. In the present study, the analogue des-Trp^1-BPP-BrachyNH$_2$ was 3.2-fold more potent in inhibition of ACE activity compared to BPP-BrachyNH$_2$. On the other hand, the analogue des-Pro^8-BPP-BrachyNH$_2$ was 29.5-fold less active when IC_{50} values were compared with those of BPP-BrachyNH$_2$. In this sense, in order to better investigate how BPP-BrachyNH$_2$ interacts with ACE, *in silico* approaches based on molecular dynamics simulations were applied.

Previous studies have reported the importance of the proline residue in the inhibition of ACE activity. Likewise, the ACE inhibitory activity induced by the antihypertensive drug captopril is based on the imitation of the proline residue in angiotensin-I. When captopril binds to ACE, the conversion of angiotensin-I into angiotensin-II is decreased, and the production of bradykinin is increased [10]. In the present work, MD simulations demonstrated that the ACE/BBP-BrachyNH$_2$ complex showed lower binding and van der Wall energies then the ACE/des-Pro$_8$-BPP-BrachyNH$_2$ complex, therefore being more stable. The large difference in the binding energy is due to the fact that a large part of des-Pro^8-BPP-BrachyNH$_2$ was not in contact with the active catalytic site of ACE. Initially, docking studies did not reveal the lack of interaction and it was only found by MD simulations. This finding agree with the study byFernandez et al. (2003), where the structural basis of the lisinopril-binding specificity in N- and C-domains of human somatic ACE was assessed. They reported important C-terminal proline hydrophobic accommodations in ACE/lisinopril complex [41]. Therefore, the markedly low efficiency of the des-Pro^8-BPP-BrachyNH$_2$ as ACE inhibitor found in the present study reinforces the importance of the characteristic C-terminal proline residue in BPPs for the inhibition of ACE activity.

The N-terminal tryptophan residue (Trp^1) from BPP-BrachyNH$_2$ is linked to a proline residue (Pro^2). Tryptophan-proline complexes are well known to possess very stable interactions due to the contact between nitrogen heteroatom of proline and the aromatic chain of tryptophan. The stabilization energy of this complex is large and structurally important in interactions and recognition processes of proteins and peptides [42]. In the present study, *in silico* and *in vitro* studies were also performed to predict toxicological targets and effects. The *in silico* predicted LD_{50} values of des-Trp^1-BPP-BrachyNH$_2$ for the acute and chronic toxicity in rats administered orally seem to be slightly lower than LD_{50} values for BPP-BrachyNH$_2$ and des-Pro^1-BPP-BrachyNH$_2$, probably indicating a higher toxic effect. This is supported by the observed increase in toxicity of des-Trp^1-BPP-BrachyNH$_2$ in murine peritoneal macrophages compared with BPP-BrachyNH$_2$. Thus, the possible lack of structural stabilization due to the removal of Trp^1 from the BPP-BrachyNH$_2$ might explain this increase in toxicity.

The C-terminal proline residue (Pro^8) from BPP-BrachyNH$_2$ is linked to a serine residue (Ser^7). The serine-proline motif is essentially found in a large number of biologically active peptides. Considered as a constrained analogue of serine, its use is mostly advantageous in conformational binding studies, frequently related to improvement in physical properties or different biological activities of peptides, as well as the design of new peptidomimetics [43,44]. In the present study, the peptide des-Pro^8-BPP-BrachyNH$_2$ was 190-fold less cytotoxic than BPP-BrachyNH$_2$. Similar results were found for ACE inhibition, where the removal of the C-terminal proline residue also decreased the inhibition of ACE activity with 29.4 times compared to BPP-BrachyNH$_2$. In this sense, putative interactions between peptide and mammalian cells might be impaired after removal of the C-terminal Pro^8 residue from BPP-BrachyNH$_2$, and then promotes a marked decrease in cytotoxicity.

In conclusion, the aminoacid sequence of BPP-BrachyNH$_2$ is essential for its ACE inhibitory activity and associated with an acceptable toxicological profile. The perspective of the interactions of BPP-BrachyNH$_2$ with ACE found in the present study can be used for development of drugs with differential therapeutic profile than current ACE inhibitors.

Author contributions

Conceived and designed the experiments: ACM, MPB, NV, EBO, FAAC, RMR, JRSAL. Performed the experiments: DDRA, AGV, LAN, ACM, AP, MMMA, NV. Analyzed the data: DDRA, AGV, AP, MPB, RMR, JRSAL. Contributed with reagents/materials/analysis tools: EBO, CDM, PG, EBO, FCAL, YPM, FAAC, US, MPB. Wrote the paper: DDRA, AGV, RMR, US, JRSAL. Provided the English proofreading: DDRA, MPB, US. The manuscript was written through contributions of all authors. All authors have given approval to the final version of the manuscript.

Funding sources

This work was funded by Coordenação de Aperfeiçoamento de Pessoal de Nível Superior, Brazil (Grant BEX 2883/15-5); Fundação de Amparo à Pesquisa do Estado de São Paulo - FAPESP, Brazil (Grants no. 14/02282e02286 and no. 16/18023-5); Fundação de Amparo à Pesquisa do Estado do Piauí - FAPEPI, Brazil (Agreement CAPES-FAPEPI no. 008/2012); and Fundação para a Ciência e Tecnologia - FCT, Portugal (Grants no. IF/00092/2014, SFRH/BD/97995/2013 and UID/QUI/50006/2013).

Acknowledgments

DDRA are grateful to FAPEPI (Edital no. 008/2012, *Acordo* CAPES-FAPEPI) and CAPES Foundation (Bolsista CAPES-PDSE e Processo no BEX 2883/15-5) for the financial support. ACM is grateful to FAPESP (Grants No. 14/02282-6 and No. 16/18023-5). RMR gives special thanks to Profa. Ana Amélia de Carvalho Melo Cavalcante, Ph.D. RMR thanks Brazilian Center of High Performance Processing (CENAPAD-UFC). RMR thanks the partnership of Prof. Fábio de Jesus Lima Gomes, Ph.D., of the Laboratory of Innovations on Multimedia Systems (LIMS). NV thanks *Fundação para a Ciência e a Tecnologia* - FCT for IF2014 position and project grant IF/00092/2014. PG thanks FCT for funding through UID/QUI/50006/2013. AP is gratefully to FCT by her grant SFRH/BD/97995/2013, financed by POPHeQ-RENeTipologia 4.1eFormação Avançada, subsidized by *Fundo Social Europeu and Ministério da Ciência, Tecnologia e Ensino Superior*. The work at REQUIMTE/LAQV received financial support from the European Union (FEDER funds through COMPETE) and National Funds (FCT) through project UID/QUI/50006/2013. The authors wish to acknowledge to Materials Center of the University of Porto (CEMUP) for MALDI-TOF mass spectrometry facilities.

Supplementary data

https://ars.els-cdn.com/content/image/1-s2.0-S0223523417306220-mmc3.pdf
https://ars.els-cdn.com/content/image/1-s2.0-S0223523417306220-mmc1.pdf
https://ars.els-cdn.com/content/image/1-s2.0-S0223523417306220-mmc2.pdf

References

[1] S.H. Ferreira, A bradykinin-potentiating factor (BPF) present in the venom of *Bothrops jararaca*, Br. J. Pharmacol. Chemother. 24 (1965) 163e169, http://dx.doi.org/10.1111/j.1476-5381.1965.tb02091.x.

[2] A.C.M. Camargo, D. Ianzer, J.R. Guerreiro, S.M.T. Serrano, Bradykinin-potenti- ating peptides: beyond captopril, Toxicon 59 (2012) 516e523, http://dx.doi.org/10.1016/j.toxicon.2011.07.013.

[3] K.L.P. Morais, D. Ianzer, J.R.R. Miranda, R.L. Melo, J.R. Guerreiro, R.A.S. Santos,
H. Ulrich, C. Lameu, Proline rich-oligopeptides: diverse mechanisms for anti- hypertensive action, Peptides 48 (2013) 124e133, http://dx.doi.org/10.1016/j.peptides.2013.07.016.

[4] J.M. Conlon, Bradykinin-related peptides from frog skin, in: Handb. Biol. Act. Pept, Elsevier, 2006, pp. 291e294, http://dx.doi.org/10.1016/B978- 012369442-3/50047-7.

[5] D. Coates, The angiotensin converting enzyme (ACE), Int. J. Biochem. Cell Biol.
35 (2003) 769e773, http://dx.doi.org/10.1016/S1357-2725(02)00309-6.

[6] R.A.S. Gomes, L.G.V.L. Teodoro, I.C.R. Lopes, P.A. Bersanetti, A.K. Carmona,
V. Hial, Enzima conversora de angiotensina no líquido pericárdico: estudo comparativo com a atividade sérica, Arq. Bras. Cardiol. 91 (2008) 172e178, http://dx.doi.org/10.1590/S0066-782X2008001500006.

[7] M.C. Araujo, R.L. Melo, M.H. Cesari, M.A. Juliano, L. Juliano, A.K. Carmona, Peptidase specificity characterization of C- and N-terminal catalytic sites of angiotensin I-converting enzyme, Biochemistry 39 (2000) 8519e8525. http:// doi.org/10.1021/bi9928905. (Accessed 21 February 2017).

[8] I. Schechter, A. Berger, On the size of the active site in proteases. I. Papain, Biochem. Biophys. Res. Commun. 27 (1967) 157e162, http://dx.doi.org/10.1016/S0006-291X(67)80055-X.

[9] D.D.R. Arcanjo, A.G. Vasconcelos, S.G. Comerma-Steffensen, J.R. Jesus, L.P. Silva,
O.R. Pires, C.M. Costa-Neto, E.B. Oliveira, L. Migliolo, O.L. Franco, C.B.A. Restini,
M. Paulo, L.M. Bendhack, M.P. Bemquerer, A.P. Oliveira, U. Simonsen,
J.R.S.A. Leite, A novel vasoactive proline-rich oligopeptide from the skin secretion of the frog Brachycephalus ephippium, PLoS One 10 (2015) e0145071,
http://dx.doi.org/10.1371/journal.pone.0145071.

[10] D.W. Cushman, M.A. Ondetti, Design of angiotensin converting enzyme in- hibitors, Nat. Med. 5 (1999) 1110e1112, http://dx.doi.org/10.1038/13423.

[11] R.J. Lewis, M.L. Garcia, Therapeutic potential of venom peptides, Nat. Rev.
Drug Discov. 2 (2003) 790e802, http://dx.doi.org/10.1038/nrd1197.

[12] G.B. Fields, R.L. Noble, Solid phase peptide synthesis utilizing 9- fluorenylmethoxycarbonyl amino acids, Int. J. Pept. Protein Res. 35 (1990) 161e214, http://dx.doi.org/10.1111/j.1399-3011.1990.tb00939.x.

[13] M.J. Frisch, G.W. Trucks, H.B. Schlegel, G.E. Scuseria, M.A. Robb,
J.R. Cheeseman, G. Scalmani, V. Barone, G.A. Petersson, H. Nakatsuji, X. Li,
M. Caricato, A. Marenich, J. Bloino, B.G. Janesko, R. Gomperts, B. Mennucci,
H.P. Hratchian, J.V. Ortiz, A.F. Izmaylov, J.L. Sonnenberg, D. Williams-Young,
F. Ding, F. Lipparini, F. Egid, J. Goings, B. Peng, A. Petrone, T. Henderson,
D. Ranasinghe, V.G. Zakrzewski, J. Gao, N. Rega, G. Zheng, W. Liang, M. Hada,
M. Ehara, K. Toyota, R. Fukuda, J. Hasegawa, M. Ishida, T. Nakajima, Y. Honda,
O. Kitao, H. Nakai, T. Vreven, K. Throssell, J.A. Montgomery Jr., J.E. Peralta,
F. Ogliaro, M. Bearpark, J.J. Heyd, E. Brothers, K.N. Kudin, V.N. Staroverov,
T. Keith, R. Kobayashi, J. Normand, K. Raghavachari, A. Rendell, J.C. Burant,
S.S. Iyengar, J. Tomasi, M. Cossi, J.M. Millam, M. Klene, C. Adamo, R. Cammi,
J.W. Ochterski, R.L. Martin, K. Morokuma, O. Farkas, J.B. Foresman, D.J. Fox, Gaussian 09, Revision A.02, 2016. http://gaussian.com/g09citation/.

[14] J.J. Stewart, MOPAC: a semiempirical molecular orbital program, J. Comput. Aided. Mol. Des. 4 (1990) 1e105. http://www.ncbi.nlm.nih.gov/pubmed/ 2197373. (Accessed 6 February 2017).

[15] A.W. Schüttelkopf, D.M.F. van Aalten, PRODRG: a tool for high-throughput crystallography of proteineligand complexes, Acta Crystallogr. Sect. D. Biol. Crystallogr. 60 (2004) 1355e1363, http://dx.doi.org/10.1107/ S0907444904011679.

[16] D.S. Goodsell, G.M. Morris, A.J. Olson, Automated docking of flexible ligands: applications of autodock, J. Mol. Recognit. 9 (1996) 1e5, http://dx.doi.org/10.1002/(SICI)1099-1352(199601)9, 1<1::AID-JMR241>3.0.CO;2e6.

[17] D.S. Goodsell, Computational docking of biomolecular complexes with Auto- Dock, in: E.A. Golemis, P.D.

Adams (Eds.), Protein-protein Interact. A Mol. Cloning Man, Second, Cold Spring Harbor Laboratory Press, New York, 2005, pp. 885e892.

[18] G.M. Morris, R. Huey, A.J. Olson, Using AutoDock for ligand-receptor docking, in: Curr. Protoc. Bioinforma, John Wiley & Sons, Inc, Hoboken, NJ, USA, 2008, http://dx.doi.org/10.1002/0471250953.bi0814s24, p. 8.14.1-8.14.40.

[19] M.F. Sanner, Python: a programming language for software integration and development, J. Mol. Graph. Model 17 (1999) 57e61. http://www.ncbi.nlm.nih.gov/pubmed/10660911. (Accessed 6 February 2017).

[20] J. Gasteiger, M. Marsili, Iterative partial equalization of orbital electro- negativityda rapid access to atomic charges, Tetrahedron 36 (1980) 3219e3228, http://dx.doi.org/10.1016/0040-4020(80)80168-2.

[21] G.M. Morris, D.S. Goodsell, R.S. Halliday, R. Huey, W.E. Hart, R.K. Belew,

A.J. Olson, Automated docking using a Lamarckian genetic algorithm and an empirical binding free energy function, J. Comput. Chem. 19 (1998) 1639e1662, http://dx.doi.org/10.1002/(SICI)1096-987X(19981115)19, 14<1639::AID-JCC10>3.0.CO;2-B.

[22] F.J. Solis, R.J.-B. Wets, Minimization by random search techniques, Math. Oper. Res. 6 (1981) 19e30. http://www.jstor.org/stable/3689263. (Accessed 6 February 2017).

[23] C. Oostenbrink, A. Villa, A.E. Mark, W.F. Van Gunsteren, A biomolecular force field based on the free enthalpy of hydration and solvation: the GROMOS force-field parameter sets 53A5 and 53A6, J. Comput. Chem. 25 (2004) 1656e1676, http://dx.doi.org/10.1002/jcc.20090.

[24] D. van der Spoel, E. Lindahl, B. Hess, the GROMACS development team, GROMACS User Manual, 2014, version 4.6.7. www.gromacs.org.

[25] H.J.C. Berendsen, J.P.M. Postma, W.F. van Gunsteren, J. Hermans, Interaction Models for Water in Relation to Protein Hydration, Springer Netherlands, 1981, pp. 331e342, http://dx.doi.org/10.1007/978-94-015-7658-1_21.

[26] S. Nosé, M.L. Klein, Constant pressure molecular dynamics for molecular

systems, Mol. Phys. 50 (1983) 1055e1076, http://dx.doi.org/10.1080/ 00268978300102851.

[27] M. Parrinello, A. Rahman, Polymorphic transitions in single crystals: a new molecular dynamics method, J. Appl. Phys. 52 (1981) 7182e7190, http://dx.doi.org/10.1063/1.328693.

[28] B. Hess, H. Bekker, H.J.C. Berendsen, J.G.E.M. Fraaije, LINCS: a linear constraint solver for molecular simulations, J. Comput. Chem. 18 (1997) 1463e1472, http://dx.doi.org/10.1002/(SICI)1096-987X(199709)18, 12<1463::AID- JCC4>3.0.CO;2-H.

[29] T. Darden, D. York, L. Pedersen, Particle mesh Ewald: an *N* ,log(*N*) method for

Ewald sums in large systems, J. Chem. Phys. 98 (1993) 10089e10092, http:// dx.doi.org/10.1063/1.464397.

[30] R.A. Laskowski, M.B. Swindells, LigPlotþ: multiple ligandeprotein interaction diagrams for drug discovery, J. Chem. Inf. Model 51 (2011) 2778e2786, http:// dx.doi.org/10.1021/ci200227u.

[31] R.M. Ramos, J.M. Perez, L.A. Baptista, H.L.N. de Amorim, Interaction of wild type, G68R and L125M isoforms of the arylamine-N-acetyltransferase from *Mycobacterium tuberculosis* with isoniazid: a computational study on a new possible mechanism of resistance, J. Mol. Model 18 (2012) 4013e4024, http:// dx.doi.org/10.1007/s00894-012-1383-6.

[32] R. Kumari, R. Kumar, A. Lynn, A. Lynn, *g_mmpbsa* da GROMACS tool for high- throughput MM-PBSA calculations, J. Chem. Inf. Model 54 (2014) 1951e1962, http://dx.doi.org/10.1021/ci500020m.

[33] N.A. Baker, D. Sept, S. Joseph, M.J. Holst, J.A. McCammon, Electrostatics of nanosystems: application to microtubules and the ribosome, Proc. Natl. Acad. Sci. U. S. A. 98 (2001) 10037e10041, http://dx.doi.org/10.1073/ pnas.181342398.

[34] A. Pedretti, L. Villa, G. Vistoli, VEGAean open platform to develop chemo-bio- informatics applications, using plug-in architecture and script programming,

J. Comput. Aided. Mol. Des. 18 (2004) 167e173. http://www.ncbi.nlm.nih.gov/ pubmed/15368917. (Accessed 20 October 2016).

[35] D.E.V. Pires, T.L. Blundell, D.B. Ascher, pkCSM: predicting small-molecule pharmacokinetic and toxicity properties using graph-based signatures, J. Med. Chem. 58 (2015) 4066e4072, http://dx.doi.org/10.1021/ acs.jmedchem.5b00104.

[36] K.A.F. Rodrigues, L.V. Amorim, C.N. Dias, D.F.C. Moraes, S.M.P. Carneiro,

F.A.A. Carvalho, Syzygium cumini (L.) Skeels essential oil and its major con- stituent a-pinene exhibit anti-Leishmania activity through immunomodula- tion in vitro, J. Ethnopharmacol. 160 (2015) 32e40, http://dx.doi.org/10.1016/ j.jep.2014.11.024.

[37] D.D.R. Arcanjo, A.C. Mafud, A.G. Vasconcelos, J.C. da Silva-Filho, M.P.M. Amaral,

L.M. Brito, M.P. Bemquerer, S.A.S. Kückelhaus, A. Plácido, C. Delerue-Matos,

N. Vale, Y.P. Mascarenhas, F.A.A. Carvalho, A.P. Oliveira, J.R.S.A. Leite, In Silico, In vitro and in vivo toxicological assessment of BPP-BrachyNH2, a vasoactive proline-rich oligopeptide from Brachycephalus ephippium, Int. J. Pept. Res. Ther. (2016),

http://dx.doi.org/10.1007/s10989-016-9564-2.

[38] S.E. Lofgren, L.C. Miletti, M. Steindel, E. Bachère, M.A. Barracco, Trypanocidal and leishmanicidal activities of different antimicrobial peptides (AMPs) iso- lated from aquatic animals, Exp. Parasitol. 118 (2008) 197e202, http://dx.doi.org/10.1016/j.exppara.2007.07.011.

[39] C.J. Yates, G. Masuyer, S.L.U. Schwager, M. Akif, E.D. Sturrock, K.R. Acharya, Molecular and thermodynamic mechanisms of the chloride-dependent hu- man angiotensin-I-converting enzyme (ACE), J. Biol. Chem. 289 (2014) 1798e1814, http://dx.doi.org/10.1074/jbc.M113.512335.

[40] E.F. Pettersen, T.D. Goddard, C.C. Huang, G.S. Couch, D.M. Greenblatt, E.C. Meng, T.E. Ferrin, UCSF Chimerada visualization system for exploratory research and analysis, J. Comput. Chem. 25 (2004) 1605e1612, http://dx.doi.org/10.1002/jcc.20084.

[41] J.H. Fernandez, M. a F. Hayashi, A.C.M. Camargo, G. Neshich, Structural basis of the lisinopril-binding specificity in N- and C-domains of human somatic ACE, Biochem. Biophys. Res. Commun. 308 (2003) 219e226, http://dx.doi.org/ 10.1016/S0006-291X(03)01363-9.

[42] L. Biedermannova, K.E. Riley, K. Berka, P. Hobzaa, J. Vondrasek, Another role of proline: stabilization interactions in proteins and protein complexes con- cerning proline and tryptophane, Phys. Chem. Chem. Phys. 10 (2008) 6350e6359, http://dx.doi.org/10.1039/b805489b.

[43] A. Ammazzalorso, B. Filippis, C. Maccallini, M. Pierini, Synthetic strategies to serine-proline chimeras: an overview, Curr. Bioact. Compd. 12 (2016) 136e145, http://dx.doi.org/10.2174/1573407212666160511150017.

[44] B. Song, M.G. Bomar, P. Kibler, K. Kodukula, A.K. Galande, The serine-proline turn: a novel hydrogen-bonded template for designing peptidomimetics, Org. Lett. 14 (2012) 732e735, http://dx.doi.org/10.1021/ol203272k.